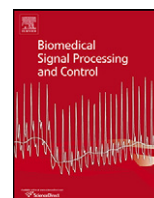




Contents lists available at ScienceDirect

## Biomedical Signal Processing and Control

journal homepage: [www.elsevier.com/locate/bspc](http://www.elsevier.com/locate/bspc)



# Discovery of multiple level heart-sound morphological variability resulting from changes in physiological states

Svetlana Kofman<sup>a</sup>, Amitai Bickel<sup>b</sup>, Arie Eitan<sup>b</sup>, Atalia Weiss<sup>b</sup>, Noam Gavriely<sup>c</sup>, Nathan Intrator<sup>a,\*</sup>

<sup>a</sup> School of Computer Science, Tel-Aviv University, Tel-Aviv, Israel

<sup>b</sup> Department of Surgery, The Western Galilee hospital, Nahariya, Israel

<sup>c</sup> Rappaport Faculty of Medicine, Technion-Israel Institute of Technology, Haifa, Israel

### ARTICLE INFO

#### Article history:

Received 12 December 2010

Received in revised form 19 June 2011

Accepted 5 August 2011

Available online xxx

#### Keywords:

Phonocardiography

Cluster analysis

Classification

Cardiac monitoring

Cardiopulmonary interaction

### ABSTRACT

Heart sounds carry information about the mechanical activity of the cardiovascular system. This information includes the specific physiological state of the subject, and short term variability related to the respiratory cycle. The interpretation of the sounds and extraction of changes in the physiological state, while monitoring short term variability is still an open problem and is the subject of this paper.

We present a novel computational framework for analysis of data with multi-level variability, caused by externally induced changes. The framework presented includes an initial clustering of the first heart sound (S1) according to the morphology, and further aggregation of clusters into *super-clusters*. The clusters and *super clusters* are two methods of data segmentation, each reflecting a different level of variability in the data.

The framework is applied to heart sounds recorded during laparoscopic surgeries of six patients. Procedures of this kind include anesthesia and abdominal insufflation, which together with the respiratory cycle, induce changes to the heart sound signal. We demonstrate a separation of the heart sound morphology according to different physiological states. The physiological states considered are the respiratory cycle, and the stages of the surgery. We achieve results of  $90 \pm 4\%$  classification accuracy of heart beats to operation stages.

The proposed framework is general and can be used to analyze data characterized by multi-level variability for various other (biomedical) applications.

© 2011 Elsevier Ltd. All rights reserved.

## 1. Introduction

The heart sounds are generated by blood flow and closure of valves inside the beating heart. The heart sound morphology changes due to a complex interplay between pressure gradients in atria, ventricles and arteries. These affect the timing, magnitude and morphology of the produced heart sounds [1]. The resulting non-stationary signal can indirectly reflect the physiological state of the subject. It changes due to alterations in bodily state and is constantly affected by the respiratory cycle and the presence of noise.

Abdominal insufflation performed during laparoscopic surgeries and the respiratory cycle, are two processes affecting the heart sound morphology. The first changes the pressure gradients in the large veins between those located in the abdominal cavity (inferior vena cava) and in the lower limbs, thus affecting venous return to

the heart. The second changes the pressure gradients in the lungs. Both consequently affect the heart sound morphology [2,3].

When trying to recognize changes in heart sounds that are related to pathology, we encounter the problem of separating changes that occur due to the respiratory cycle from pathological events. The goal of this research is to build a clustering/classification framework that can handle both types of morphological changes and produce a robust prediction of the physiological state, independently of the large variability of heart sounds.

The heart sound is perhaps the most traditional biomedical signal, as indicated by the fact that the stethoscope is the primary instrument carried and used by physicians. This signal reflects mechanical changes in heart functionality and provides an indication of the general state of the heart in terms of rhythm and contractility. The phonocardiogram is a recording of the heart sound signal [4,5]. The heart sound signal or PCG signal of a normal heart is comprised of two distinct activities namely the first heart sound, S1 and the second heart sound, S2 (Fig. 1). S1 occurs at the end of the isometric contraction period during systole, and S2 occurs after the isovolumetric relaxation period during diastole [6].

\* Corresponding author at: School of Computer Science, Faculty of Exact Sciences, Tel-Aviv University, P.O.B. 39040, Tel-Aviv 69978, Israel.

E-mail address: [nin@tau.ac.il](mailto:nin@tau.ac.il) (N. Intrator).

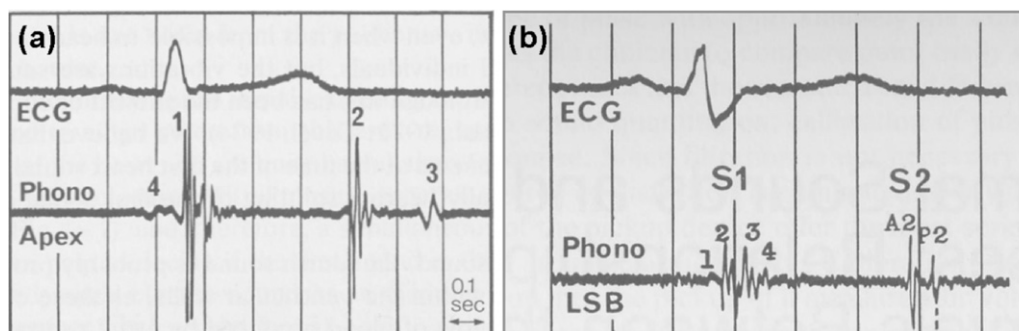


**Fig. 1.** A phonocardiogram recording of a single heart beat, showing the two major heart sounds S1 and S2, as well as S3 and S4 (a), and a detailed description of the inner structure of S1 and S2 (b), showing their subcomponents [4].

The pulmonary system plays an important part in modulating the cardiovascular mechanical activity by respiratory-induced changes of the pleural pressure, arterial resistance and venous return. Amit et al. observed significant differences between properties of S1 and S2 occurring during inspiration and expiration [3].

The field of automated analysis of the heart sound signals is relatively new. Recent technological advances in digital electronic stethoscopes, acoustic signal processing and pattern recognition methods have made possible the design of algorithms for automated heart sound segmentation and classification [7]. Research in this field often focuses on two computational problems: the segmentation of heart sounds into heart cycles [8,9] and the recognition of the heart sound components (often only S1 and S2, and sometimes also S3, S4 and murmurs) [10,11], and classification of heart sounds for recognizing cardiac pathologies [12–14].

Much research was done on the classification of different heart sounds (HS), each representing a different cardiac pathology. Heart sounds are often preprocessed by converting them to a time-frequency signal representation scheme. Methods such as short time Fourier transform, Wigner–Ville distribution, continuous wavelet transform and reduced-interference distributions have been previously applied on heart sound signals [8,15]. Classification algorithms such as multilayer perceptron networks, learning vector quantization (LVQ) [12,14], and clustering analysis [13,16] were used to classify the different heart sounds. It was shown that it is possible to achieve a high classification performance after a short training time, and thus to carry out heart sound classification in real-time [8,9].

Work by Amit et al. [1], described a framework for identifying distinct morphologies of heart sounds and classifying them into physiological states. This work focused on the effect of the respiratory cycle and the respiratory resistive load on the morphologies of S1 and S2. The framework presented in this paper builds on the analysis introduced by Amit et al.

In this work we extend the framework presented by Amit et al. Our framework analyzes heart sounds characterized by multi-level variability, caused by physiological events as well as the respiratory cycle. The extended framework enables a clear separation between morphological changes caused by the respiratory cycle, and those caused by physiological changes. We demonstrate that those physiological changes, which are extremely important for monitoring cardiac patients are better detected by the proposed method. The demonstration is done on patients undergoing laparoscopic surgeries. We further demonstrate that the method is applicable to other types of physiological changes [17].

## 2. Methods

The following computational framework analyzes data with different sources of variability, caused by externally induced changes.

The analysis of heart sound that is characterized by multi-level variability is done using extensive clustering and then fusing several clusters into super clusters based on sequential repetition of different clusters in a localized temporal region. The cluster centers are then used to construct a new data representation which enables identification and association of a new morphological signal into its corresponding physiological state. The classification framework is applied on the S1 component of the heart sound.

The computational framework consists of the following building blocks (described below in detail):

1. *Preprocessing* – preparation of a raw recorded signal for further analysis. Includes digital filtering of the acquired signal, segmentation to cardiac cycles and the extraction of the first heart sound (S1).
2. *Pattern recognition* – used to identify distinct morphological patterns. The segmented S1 components are clustered using an unsupervised learning method.
3. *Feature extraction* – the data set of S1 components is transformed to a compact representation of cluster distance space. Each beat is then represented by a vector of distances from the centers of significant clusters.
4. *Classification* – used to test the accuracy of the clustering and to determine whether the different signal morphologies revealed by clustering represent different physiological states.
5. *Super clustering* – a super cluster aggregates a subgroup of clusters within a time segment, to separate time segments with constant patterns of morphological behavior.

### 2.1. Experimental setup

Heart sound signals from six patients were recorded during upper abdominal laparoscopic surgery. Procedures of this kind affect the cardiovascular function by reducing venous return and increasing systemic vascular resistance, consequently causing decreased cardiac index, which eventually affect heart sounds [18,19].

The phonocardiogram signal was acquired from multiple recording locations. Supplementary data, such as electrocardiogram was acquired simultaneously. Five patients underwent laparoscopic cholecystectomy surgeries and a single patient underwent a hernia repair surgery. The study population consisted three males and three females, aged between 53 and 72. A detailed description of the subjects is presented in Table 1. Recording was done during 3 different phases of the surgery: following induction of anesthesia, during pneumoperitoneum and after abdominal CO<sub>2</sub> desufflation (end of pneumoperitoneum). The patients were intubated during the surgery, meaning they had a constant respiratory

**Table 1**  
 Test subject description.

Subject	Gender	Age	Cardiac/vascular diseases	Surgery	S1 beats used
BU	F	53	None	Lap. cholecystectomy	781
ZU	M	55	None	Lap. cholecystectomy	298
SO	M	68	Ischemic heart disease, hypertension	Lap. cholecystectomy	573
TA	M	59	None	Rep. hernia	2931
NA	F	60	Hypertension	Lap. cholecystectomy	657
HI	F	72	Ischemic heart disease	Lap. cholecystectomy	778

rate. Each recording took at least 30 s. The recordings were class labeled according to stages of the surgery.

### 2.2. Signal representation and preprocessing

Details of the phonocardiogram recording are provided in Amit et al. [16]. Following amplification, the heart sounds were filtered with a digital band pass filter in the frequency range of 20–250 Hz, where the bulk of the heart sound energy is found. The signal was then partitioned into cardiac cycles using the peaks of the ECG-QRS complexes as reference points. The signal segment containing the first heart sound, S1, was defined from the beginning of the QRS peak to 200 ms after the QRS peak. S1 signals were extracted from each cardiac cycle, standardized and aggregated for further processing. Segments with peaks significantly below or above average were recognized as noisy or invalid segments and were filtered out. The filtered heart sound signal and the S1 segments of it are shown in Fig. 2.

### 2.3. Hierarchical clustering

Hierarchical clustering is an unsupervised learning method, which requires the user to specify a measure of dissimilarity between (disjoint) groups, based on pair-wise dissimilarities in the two groups. The result is a hierarchical representation in which the clusters at each level of the hierarchy are created by merging clusters at the next lower level. At the lowest level, each cluster contains a single observation, at the highest level there is only one cluster containing all of the data. For recent advances in hierarchical clustering, see [20].

The hierarchical clustering used in this work is agglomerative, namely, it starts at the bottom of the hierarchical tree, and at each level merges the selected pair of clusters into a single cluster. The choice of the next two clusters to be combined is done using group average criterion, which chooses clusters such that the average

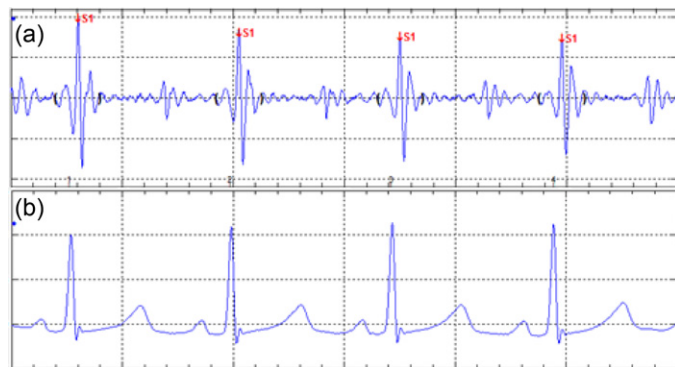


**Fig. 2.** (a) A phonocardiogram recording filtered in the frequency range of 20–250 Hz. S1 segments are shown. (b) A simultaneous recording of electrocardiogram.

dissimilarity between the groups is minimal. The distance between two clusters is defined by:

$$d_{GA}(G, H) = \frac{1}{N_G N_H} \sum_{i \in G} \sum_{j \in H} d_{ij}$$

where  $N_G, N_H$  are the respective number of observations in each group, and  $d_{ij}$  pairwise observation dissimilarity [20].

Dissimilarity is measured using a distance metric. The distance metric we used to compute the distance between observations is correlation; for  $m_i, m_j$  signals of length  $n$  we compute:

$$d_{ij} = ||m_i - m_j|| = 1 - \frac{\sum_t (m_{i,t} - \bar{m}_i)(m_{j,t} - \bar{m}_j)}{\sqrt{\sum_t (m_{i,t} - \bar{m}_i)^2} \sqrt{\sum_t (m_{j,t} - \bar{m}_j)^2}},$$

$$\text{where } \bar{m}_i = \frac{1}{n} \sum_{t=1}^n m_{i,t}$$

To obtain the desired number of clusters the hierarchical clustering tree is pruned. Observations beneath each cut are assigned to a single cluster (Fig. 3).

### 2.4. Clustering and classification framework

The clustering and classification framework presented, divides S1 heart sound signals into distinct morphological groups. Each cluster represents a unique subclass of morphologies. The accuracy of the clustering was tested on previously unseen test data using a classification algorithm.

#### 2.4.1. Clustering procedure

The input to the clustering procedure is a set of  $N$  heart sound cycles,  $B = \{(b_1, l_1), (b_2, l_2), \dots, (b_N, l_N)\}$ , where  $b_i$  is the representation of a heart sound component (e.g. S1) during a single cardiac cycle, and  $l_i$  is the associated class label  $l_i \in \{L_1, \dots, L_m\}$ . The cluster analysis procedure assigns a cluster identifier to each signal cycle,

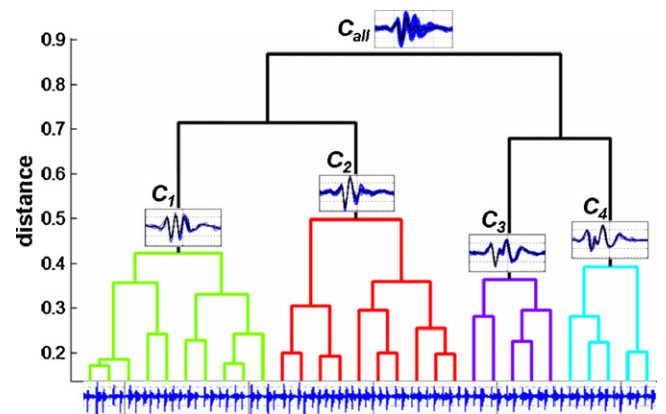


**Fig. 3.** A hierarchical clustering tree is graphically represented by a dendrogram. This illustrates the process of iteratively merging similar clusters, followed by pruning of the hierarchical tree to obtain four clusters ( $C_1, \dots, C_4$ ).

using the hierarchical clustering algorithm, producing a clustered dataset  $C = \{(b_1, c_1), (b_2, c_2), \dots, (b_N, c_N)\}$ , where  $c_i \in \{1, \dots, M\}$  are arbitrary cluster identifiers. Using this notation, a cluster  $C_j$  is the set of signal cycles with cluster identifier  $c_j$ :  $C_j = \{i | (b_i, c_j) \in C\}$ . The center of a cluster  $C_j$  is a weighted average of the clusters elements, in which each signal cycle is weighted by its similarity to the clusters arithmetic mean:

$\bar{C}_j = \sum_{i \in C_j} w_i b_i$ ,  $w_i = 1 - D(b_i, (\sum_{i \in C_j} b_i / |C_j|))$ , where  $D$  is a distance function with a maximum distance of 1 [16].

Clusters that contain more than a certain minimal portion of the heart beats in a label are denoted as *significant clusters*, i.e. cluster  $C_j$  is *significant* if there is a label  $L_i$  such that  $|\{b_k | (b_k, L_i) \in B \text{ and } (b_k, c_j) \in C\}| > |\{b_k | (b_k, L_i) \in B\}| \cdot \beta$ . (In this experiment  $\beta$  is set to 0.1.) Such a definition of a *significant cluster* prevents the state when a class label has no representation of its dominant clusters in the significant clusters set due to its small size in relation to other class labels.

Insignificant clusters are created due to noise or short term, singular physiological events (e.g. the process of abdominal insufflation causes the creation of multiple clusters). Those clusters are eliminated by merging them into significant clusters. Each beat  $b_i$  from an insignificant cluster is moved to a significant cluster  $C_j$  such that  $d_j^i = D(b_i, \bar{C}_j)$  is minimal. Cluster centers are recalculated after the merging process.

#### 2.4.2. Feature extraction

The centers of the significant clusters provide a compact representation of the morphological variability in the entire dataset. Furthermore, a signal beat  $b_i$  can be efficiently characterized by a vector of distances from the centers of the significant clusters.  $\vec{d}^i = (d_1^i, d_2^i, \dots, d_M^i)$ ,  $d_j^i = D(b_i, \bar{C}_j)$ . The classification algorithm is applied in this new feature space [1].

#### 2.4.3. Classification algorithm

The classification algorithm determines the accuracy of the clustering procedure. The algorithm attempts to predict class labels of heart beats in a previously unseen test set, using their representation in cluster distance space.

The data set  $B$  is divided into subsets  $B^{train}$  and  $B^{test}$ . Only  $B^{train}$  is used in the clustering procedure.  $B^{test}$  is used to measure the correctness of the clustering.

The division of data set  $B$  to  $B^{train}$  and  $B^{test}$  is performed separately for each class label  $L_i$ . The group  $B^{train}$  is defined as a subgroup of  $B^{train}$ , where all the heart beats belong to class label  $L_i$  ( $B_i^{train}$  is defined similarly).  $B_i^{train}$  is constructed in the following way: the group  $B_i = \{b_k | (b_k, L_i) \in B\}$  is divided to  $r$  ( $r=5$ ) equal subgroups, each containing consecutive beats from  $B_i$ :  $B_i = B_i^1 \cup B_i^2 \cup \dots \cup B_i^r$ . Those subgroups are divided equally between  $B_i^{train}$  and  $B_i^{test}$ :

$$B_i^{train} = \bigcup_{j=1}^{\lceil r/2 \rceil} B_i^{2j-1}, \quad B_i^{test} = \bigcup_{j=1}^{\lceil r/2 \rceil} B_i^{2j}$$

$$B^{train} = \bigcup_{i=1}^m B_i^{train}, \quad B^{test} = \bigcup_{i=1}^m B_i^{test}$$

For  $r=5$ ,  $B^{train}$  is 60% of the data set, and  $B^{test}$  is the remaining 40%.

The classification algorithm used is  $k$ -nearest-neighbors. This is a simple, non-parametric method, based on closest training examples in the feature space. Given a query point  $\vec{d}^0 \in B^{test}$ , and a set of labeled training points  $B^{train}$ , we find the  $k$  training points  $\vec{d}^l \in B^{train}$ ,  $l = 1, \dots, k$  closest in distance to  $\vec{d}^0$ , and then classify to label  $\tilde{l}_0 \in \{L_1, \dots, L_m\}$  using majority vote among  $k$  neighbors. Ties are broken at random [20].

Different distance metrics were tested:

1. Euclidean –  $D(i) || \vec{d}^i - \vec{d}^0 || = \sqrt{\sum_{k=1}^M (d_k^i - d_k^0)^2}$
2. Mahalanobis – based on correlations between variables by which different patterns can be identified and analyzed. It differs from Euclidean distance in that it takes into account the correlations of the data set. Defined by  $D(\vec{d}^i, \vec{d}^0) = (\vec{d}^i - \vec{d}^0)^T V^{-1} (\vec{d}^i - \vec{d}^0)$  where  $V$  the covariance matrix of  $\vec{d}^i$  and  $\vec{d}^0$  [20].

The clustering and classification outline is summarized below: Let  $B$  be the data set of a single patient.

1. Split data set  $B$  is into subsets  $B^{train}$  and  $B^{test}$ .
2. Apply the clustering procedure on the training set  $B^{train}$ , to produce a clustered data set  $C^{train}$ .
3. For each cluster in  $C^{train}$ , calculate cluster center  $\bar{C}_j^{train}$ .
4. Determine significant clusters.
5. Eliminate insignificant clusters, by moving the heart beats in them to significant clusters.
6. Recalculate cluster centers  $\bar{C}_1^{train}, \dots, \bar{C}_M^{train}$  of significant clusters in  $C^{train}$  after the merge.
7. Transform the heart beats  $b_i \in B^{train} \cup B^{test}$  to a compact representation  $\vec{d}^i = (d_1^i, d_2^i, \dots, d_M^i)$  of distances from the centers of significant training clusters.
8. Use KNN classifier to calculate the clustering accuracy. For each beat  $b_i \in B^{test}$ , in its representation in cluster distance space, calculate

$$KNN(\vec{d}^i) = \tilde{l}_i, \quad \tilde{l}_i \in \{L_1, \dots, L_m\}$$

9. Calculate classification accuracy of the patient by averaging the classification accuracy of all the class labels:

$$CA(L_i) = \frac{|\{b^j \in B^{test} \text{ and } (b^j, L_i) \in B | \tilde{l}_j = L_i\}|}{|\{b^j \in B^{test} \text{ and } (b^j, L_i) \in B\}|}, \quad CA = \frac{\sum_{i=1, \dots, m} CA(L_i)}{m}$$

The above equation gives each class label the same weight, disregarding the number of heart beats in it.

#### 2.5. Super clustering

As mentioned before, the morphological changes in data set  $B$  are caused due to two simultaneously occurring physiological processes: the respiratory cycle and the laparoscopic surgery. Morphological changes caused by the respiratory cycle manifest as cyclic transitions of adjacent heart beats between two or more clusters. Morphological changes that are caused by the laparoscopic surgery create a new set of clusters with cyclic transitions between them (Fig. 7a). The purpose of the super clustering is to divide data set  $B$  into physiological states caused by the surgery alone.

A super cluster is defined as a segment of time, in which the heart sound cycles are characterized by a small constant set of alternating morphological behaviors. This pattern manifests as transitions between a small set of clusters, and appears as cyclic transitions between two or more clusters. The criterion for the end of a super-cluster and the beginning of the next is a change in the set of clusters adjacent heart beats belong to.

The algorithm for partitioning the time line to super clusters is based on hierarchical clustering. The input to the algorithm is the clustering result of heart sound cycles.  $C = \{(b_1, c_1), (b_2, c_2), \dots, (b_N, c_N)\}$ , where  $b_i \in B$ , is a data set of heart sound components (i.e. S1), and  $c_i \in \{1, \dots, M\}$  are arbitrary cluster identifiers.  $C$  is ordered

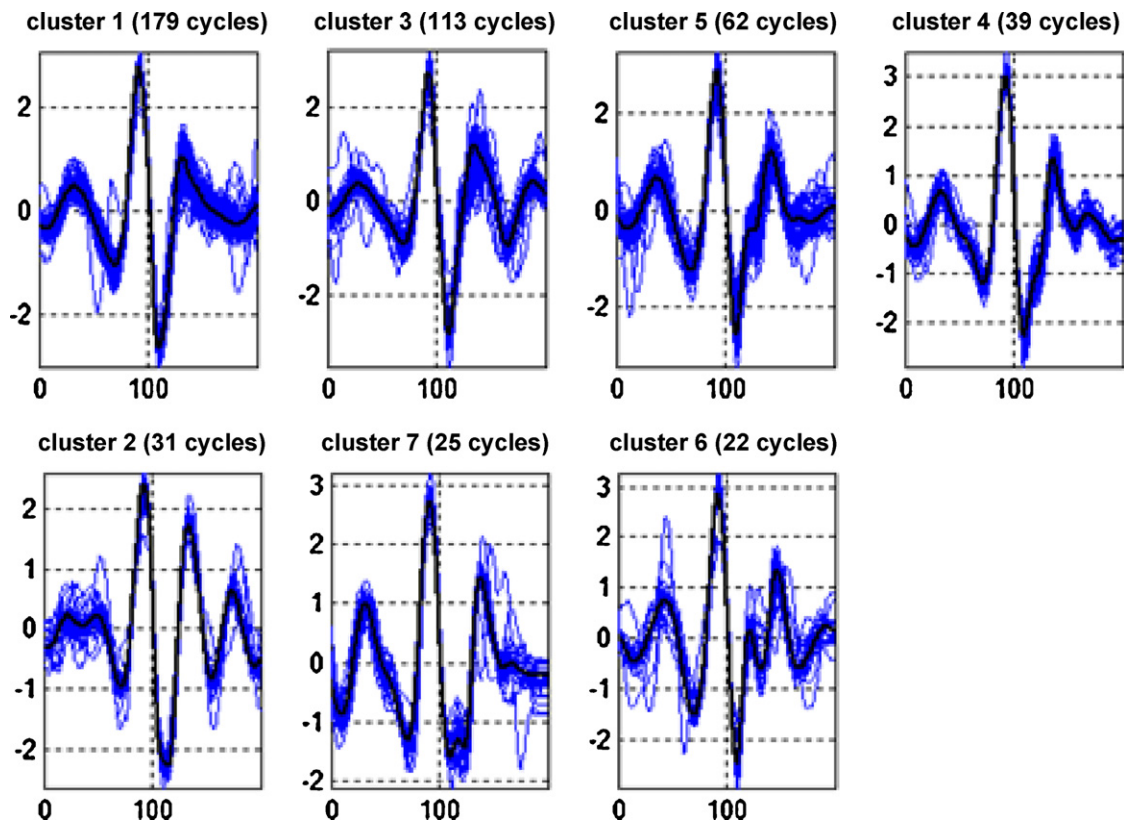


**Fig. 4.** Hierarchical clustering results of 781 S1 beats. After extracting of the first heart sound (S1), the beats were aligned using the time-shift averaging algorithm with respect to their mean. Hierarchical clustering is applied on the data with cutoff at 40 clusters. Only significant clusters are presented. The signals within each cluster are morphologically distinct, and have a small variability compared to other clusters.

by the occurrence in time of  $b_i$ . The resulting super-clusters  $SC_i$  are non overlapping subgroups of  $C$ .

$$SC_i = \{(b_j, c_j), \dots, (b_{j+t}, c_{j+t})\}$$

The super-clustering algorithm begins with the partitioning of  $C$  to windows of constant size  $d$  ( $d = 5$ ). Each window containing cluster identifiers:

$$W = \{W_1, \dots, W_k\}, \quad W_i = \{c_{d(i-1)+1}, \dots, c_{d(i-1)+d}\}$$

Hierarchical clustering is applied on the data set of windows  $W$ . The distance metric used to compare between windows is Jaccard. The Jaccard coefficient measures similarity between sample sets, and is defined as the size of the intersection divided by the size of the union of the sample sets. The Jaccard distance measures dissimilarity between sample sets, and is complementary to the Jaccard coefficient. Jaccard distance is obtained by subtracting the Jaccard coefficient from 1 [21].

$$D_{\text{Jaccard}}(W_i, W_j) = 1 - \frac{|W_i \cap W_j|}{|W_i \cup W_j|}$$

The choice of the next two clusters to be combined is done using the average criterion. The result of the hierarchical clustering algorithm is smoothed to obtain super-clusters conforming to the above definition.

### 3. Results

The clustering and classification framework was applied separately on the data set of each of the six patients. The data set was constructed from a single recording channel, chosen by its recording quality. Only the S1 component of the heart sound cycles

was used. The number of heart beats processed per subject ranged between 300 and 2930. During the preprocessing stage a mean of  $10 \pm 3.5\%$  of S1 beats were removed due to noise.

Each heart sound cycle was labeled by a class label describing the stage in the operation it was recorded in (“before operation”, “during operation”, “after operation” and intermediate labels). The number of labels ranged from 3 to 5.

The data set was divided to train and test. 60% of the S1 beats were used for training, and 40% for testing. Consecutive heart beats were selected to ensure the unbiased representation of beats occurring in different stages of the respiratory cycle, since there are respiratory-induced morphological variations of S1 [1].

Hierarchical clustering was applied on the training set, and the clustering tree obtained was pruned at 40 clusters. The number of clusters was decided upon empirically. Experiments with less clusters showed results that were not sensitive enough. Experiments with more than 40 clusters created too many small insignificant clusters. The number of significant clusters varied from 7 to 13 among subjects. Signal averaging within each cluster exhibited a small morphological variability compared to the variability of signals in different clusters, providing a more accurate description of the data (Fig. 4).

$K$ -nearest-neighbor classification was used to test the accuracy of the clustering. The algorithm attempts to predict class labels of heart beats in the previously unseen test subset, using their representation in cluster distance space. The algorithm was applied with  $K \in \{1, 3, 5\}$  and Euclidean and Mahalanobis distance metrics. The Mahalanobis distance metric was also used by Amit et al. [1] for the classification of heart sounds. It significantly improved prediction results in this study as well. The value of  $K = 1$  and the Mahalanobis distance metric gave best prediction results for the majority of the subjects. With those parameters, the classification success (CA) over

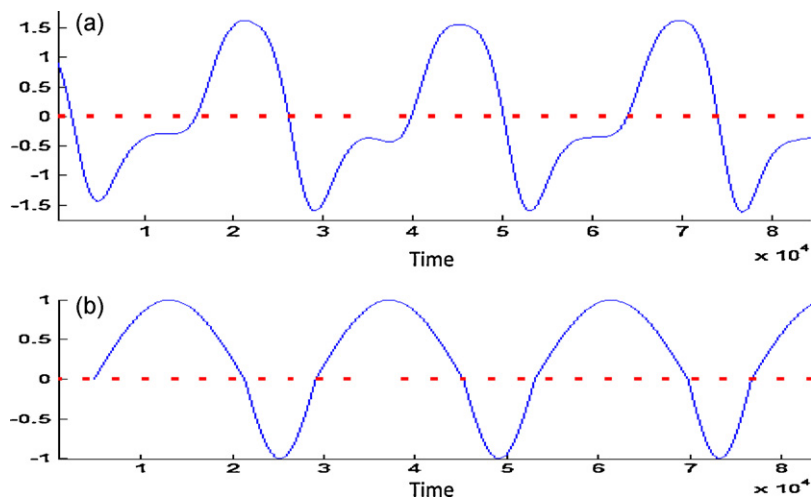


**Fig. 5.** (a) Three respiratory cycles. The lowest point of the cycle corresponds to the end of expiration and beginning of inspiration, and the highest point to the end of inspiration and the beginning of expiration. (b) Mapping of the respiratory cycle to the range 0–360. The graph shows a sinus of this map. The red intervals are times of S1 beats. (For interpretation of the references to color in this figure legend, the reader is referred to the web version of the article.)

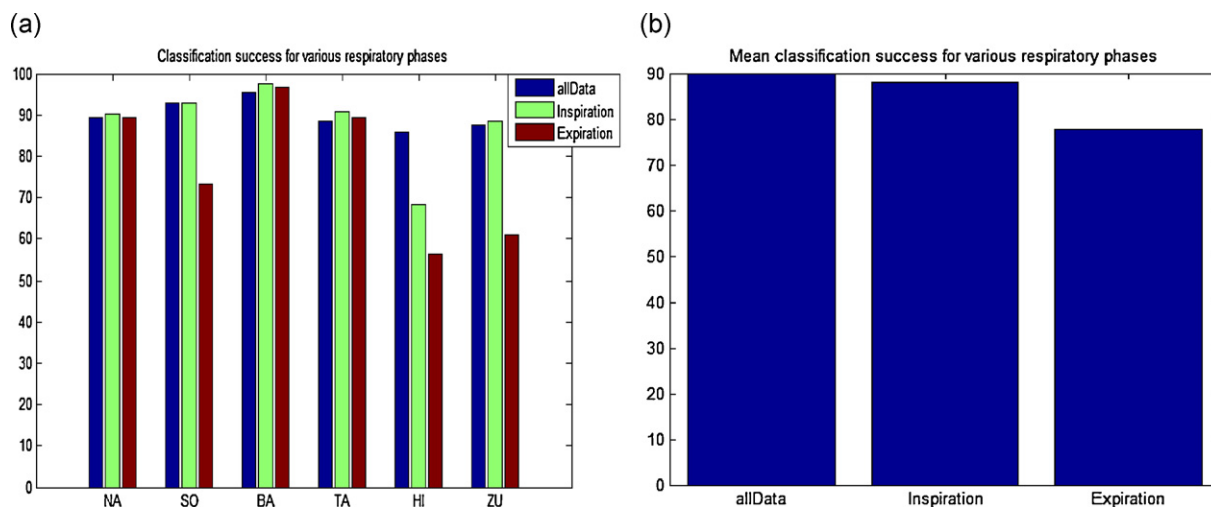


**Fig. 6.** (a) Classification accuracy (CA) values for 6 subjects for data subsets  $B_{inspiration}$ ,  $B_{expiration}$  and the entire data set. The X axis are the patients, the Y axis is the classification accuracy in percents. We can see that for 5 of 6 patients the CA of subset  $B_{inspiration}$  is slightly higher than the CA of all the data. (b) Mean classification accuracy (CA) values for data subsets  $B_{inspiration}$ ,  $B_{expiration}$  and the entire data set. Each bar is CA for five patients. Patient HI was excluded from this calculation. We can see that the mean CA is slightly better for  $B_{inspiration}$ .

6 patients was  $90 \pm 4\%$ . The CA of a patient is calculated by averaging the CA of all his class labels. This gives each class label the same weight, disregarding the number of heart beats in it. Detailed classification results can be seen in Table 2.

**Table 2**  
 Classification performance of S1 signals using the KNN algorithm.

K	Distance metric	CA
1	Euclidean	$85 \pm 5$
	Mahalanobis	<b><math>90 \pm 4</math></b>
3	Euclidean	$82 \pm 7$
	Mahalanobis	$89 \pm 6$
5	Euclidean	$78 \pm 8$
	Mahalanobis	$87 \pm 7$

Mean and standard deviation of the classification accuracy for all subjects were calculated with different parameters of the K-nearest-neighbor classification algorithm. The Mahalanobis distance metric gives significantly better results for all values of K. Best performance for  $K = 1$ .

The super clustering algorithm was further applied on the training subset. The clustered data,  $C^{train}$ , was partitioned to windows of size  $d = 5$ . The windows were clustered using hierarchical clustering algorithm, with Jaccard distance metric. The clustering tree was pruned at 10 clusters for five of the patients, and at 9 clusters for a single patient. The number of clusters was decided upon empirically. The number of super clusters was between 5 and 8.

### 3.1. Respiratory modulation within a super cluster

The respiratory cycle modulates heart sound morphology. Heart beats during high thoracic pressure (early expiration) are morphologically different from beats following high negative thoracic pressure (early inspiration) [16]. This physiological behavior should be taken into consideration when analyzing heart sound clusters. Another physiological process characterizing the data is pneumoperitoneum, which further changes thoracic pressures. This process affected the class labels of the data.

The super-cluster is a time segment in which there are transitions of heart beats among a small set of clusters. Those transitions

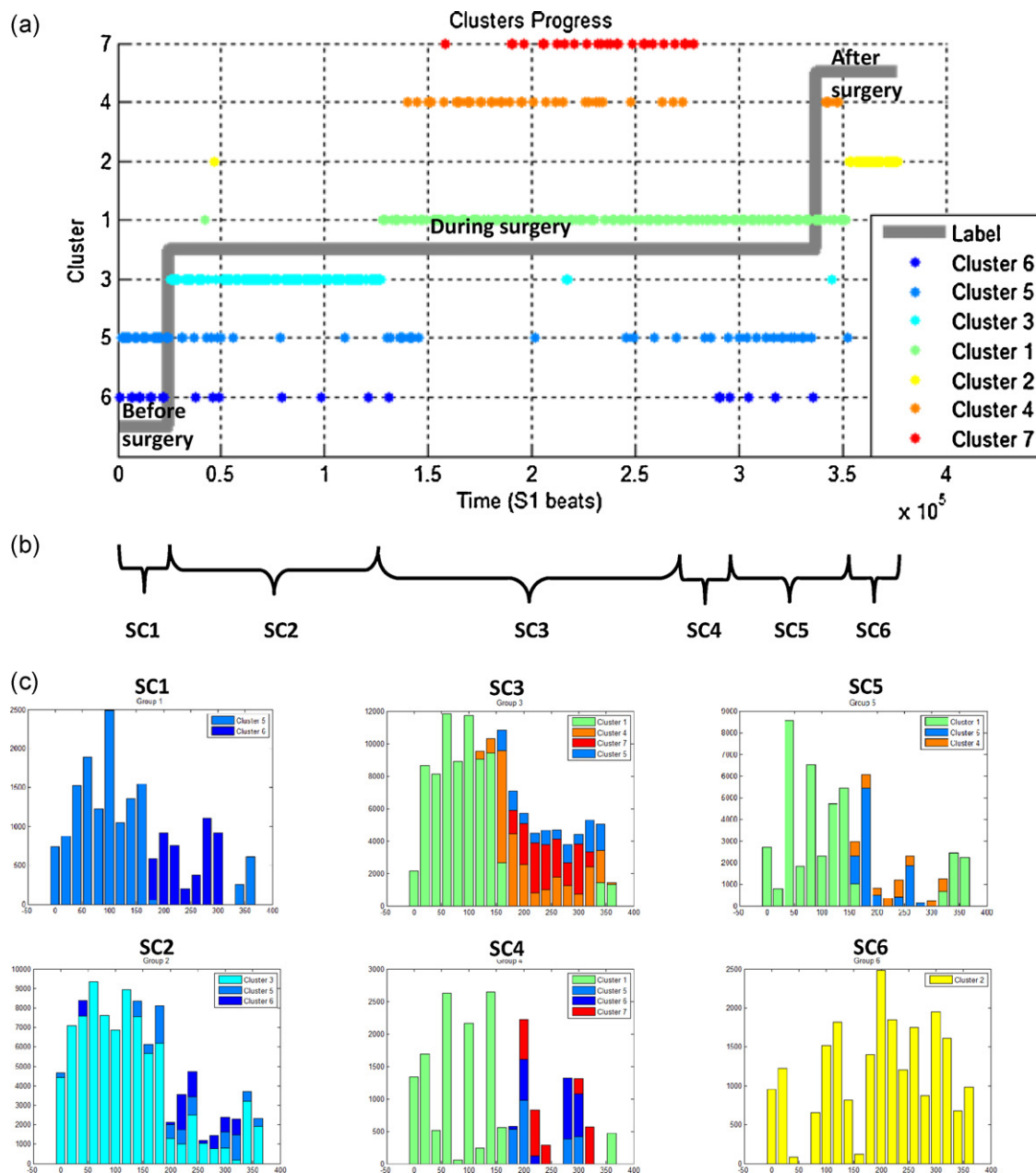


**Fig. 7.** (a) Clustering progress. The X axis is 781 S1 beats ordered by time of occurrence. Y axis are clusters. Each cluster differs both in color and in value. (b) The division of the time line to super-clusters. We can see the correlation between super clusters and class labels. (c) Histogram of the respiratory phase of the S1 beats in a super cluster. The X axis is in the range 0–360 that maps the respiratory cycle, the Y axis is the number of samples in each bar. Each color in the histogram is a different cluster within the super cluster. We can see that when there is more than one dominant cluster in a super cluster, each cluster belongs to different respiratory phase. (For interpretation of the references to color in this figure legend, the reader is referred to the web version of the article.)

can be explained by the respiratory cycle. An example of cyclic transitions can be seen in Fig. 7a. In the first label “Before operation” the S1 beats are classified periodically to both clusters 5 and 6. The morphological differences between them can be seen in Fig. 4. By showing that S1 beats in each of those clusters occur in different stages of the respiratory cycle, we show correlation between a cluster and a respiratory phase.

The respiratory signal is generated by the movement of the chest during respiration. It can be extracted from the heart sound signal by filtering it using a band pass filter in the range 0–0.5 Hz. The breathing signal is divided to respiratory cycles. The lowest point of the cycle corresponds to the end of expiration and beginning of inspiration, the highest point to the end of inspiration and

the beginning of expiration. The respiratory cycle is mapped to the range of 0–360, the sinus cycle. Inspiration corresponds to values 0–180, and expiration to 180–360 (Fig. 5).

By examining the respiratory cycle stages of S1 beats in different clusters within a single super-cluster (Fig. 7c), we observe that each cluster corresponds to a different part of the respiratory cycle, thus showing that the morphological differences within a super-cluster are caused due to respiration.

The existence of several super-clusters reveals morphological changes to the heart sounds that are caused by the alternating thoracic pressure in different stages of the operation, caused by pneumoperitoneum. Correlation between the super-clusters and class-labels only emphasizes this notion (Fig. 7b).

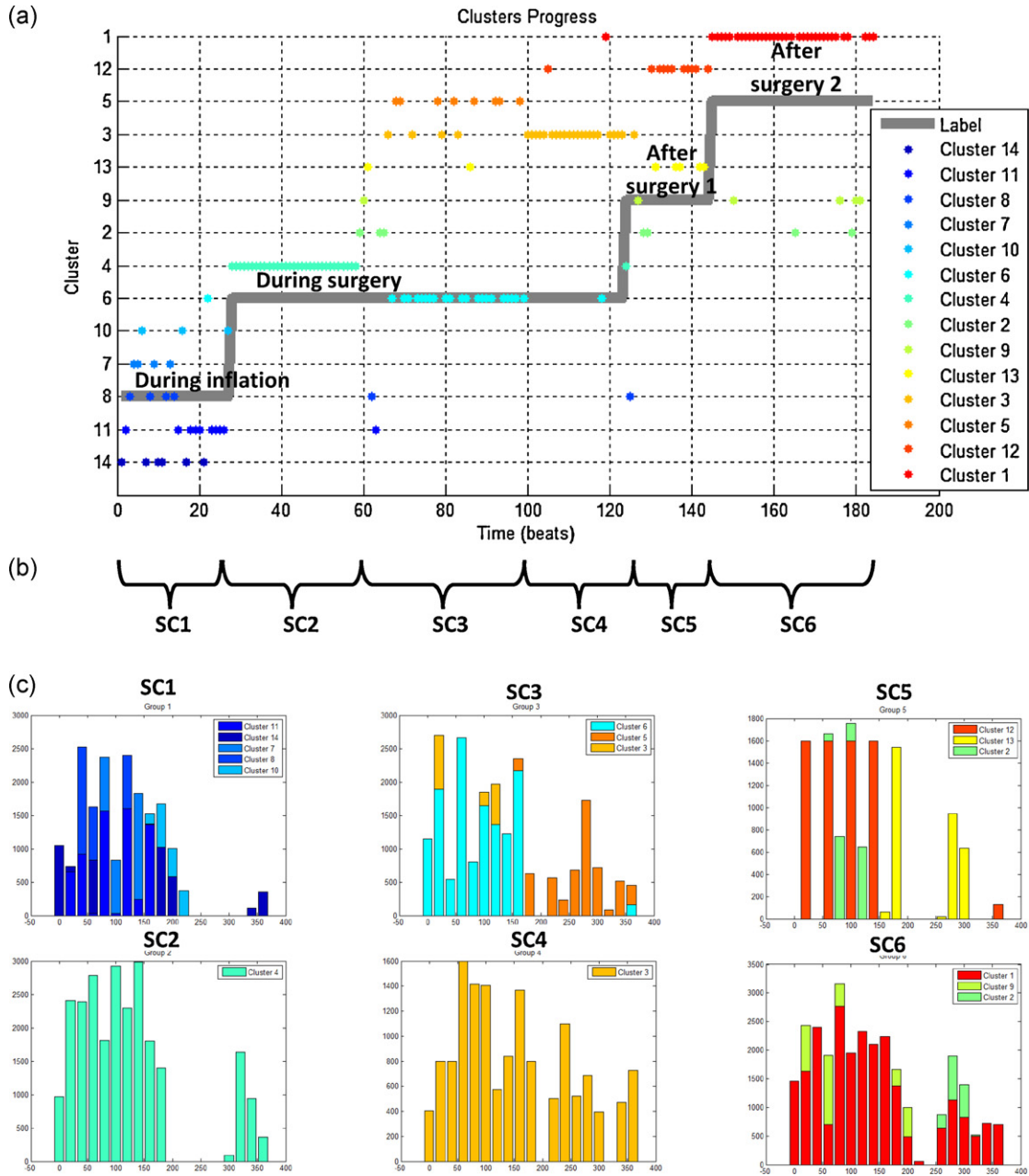


**Fig. 8.** Clustering and super clustering results for 298 S1 beats of patient ZU. This patient does not have a recording from before the surgery, only a recording from the inflation stage itself and recordings from different states of the patient during and after the surgery. For detailed explanation see Fig. 7. (For interpretation of the references to color in this figure legend, the reader is referred to the web version of the article.)

3.2. Application of the framework to subsets of the data

The respiratory cycle induces significant morphological changes to the heart sound signal [1]. Therefore, the division of the S1 beats into subsets according to the respiratory phase they occur in reduces the variability of the data. We describe an attempt to improve classification accuracy by applying the clustering and classification framework on subsets of the data, when the S1 beats in each subset belong to different phases of the respiratory cycle.

The S1 components in data set  $B$  are mapped to stages of the respiratory cycle as described in Section 3.1. Each S1 beat  $b_i$  receives a pair  $(RP_i^{start}, RP_i^{end})$  such that  $RP_i^{start}, RP_i^{end} \in [0, 360]$ , indicating the respiratory phase it begins and ends in.

The data set is divided into two subsets:

1.  $B_{inspiration}$  – heart beats  $b_i$  such that  $RP_i^{start}, RP_i^{end} \in [0, 180]$ .

2.  $B_{expiration}$  – heart beats  $b_i$  such that  $RP_i^{start}, RP_i^{end} \in [180, 360]$ .

The clustering and classification framework was applied separately on each of the data sets. The same methodology was used for the subsets as for the entire data set.  $K$ -nearest-neighbor classification algorithm was used with  $K=1$  and Mahalanobis distance metric, parameters that were shown to improve classification results. The application of the framework on the  $B_{inspiration}$  data set showed slightly better classification accuracy (CA), for most subjects. For a single subject the CA was significantly lower for this subset (Fig. 6a). Classification results of  $B_{expiration}$  did not improve CA. Mean classification accuracy for both data subsets is presented in Fig. 6b. Since the results are not unanimous among subjects, and the increase in classification accuracy is small, we cannot conclude that the use of S1 beats from the inspiration stage alone is

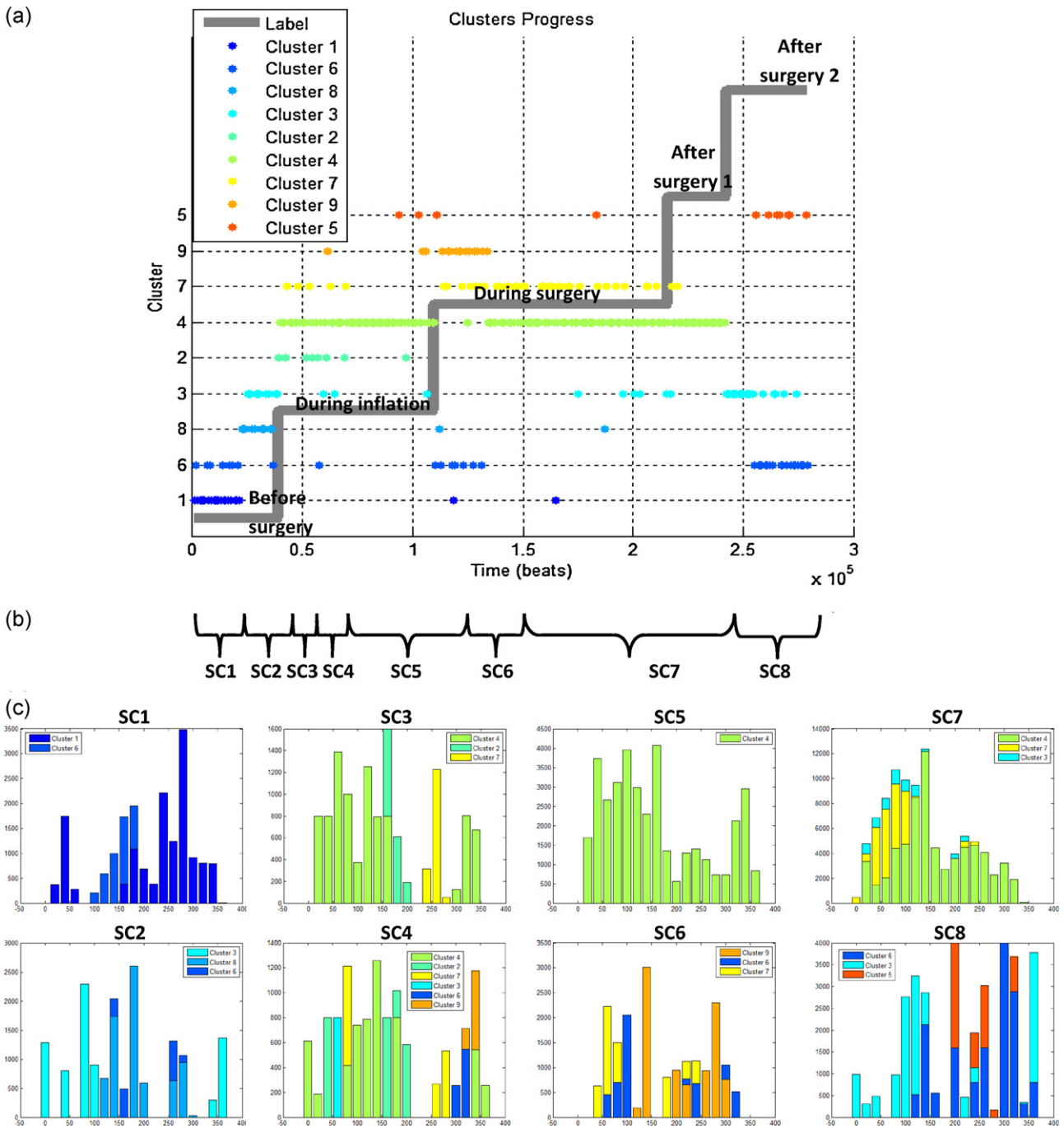


**Fig. 9.** Clustering and super clustering results for 573 S1 beats of patient SO. This patient has a recording from the inflation stage itself and recordings from different states of the patient after the surgery. For detailed explanation see Fig. 7. (For interpretation of the references to color in this figure legend, the reader is referred to the web version of the article.)

recommended. More subjects and further studying of data set division methods should be done in order to reach a decisive conclusion.

**4. Discussion and conclusions**

We have proposed a framework for the analysis of a multi-level heart sound variability. Our goal was to provide computational tools for recognizing morphological changes in the signal that occur due to pathological events, and are not related to the respiratory cycle.

The framework initially clusters the first heart sound (S1) according to its morphology, and later aggregates clusters into super clusters. The clusters and super clusters are two methods of data segmentation, each reflecting a different level of variability in the data. The results demonstrate that significant morphological changes occur during physiological state changes and in each physiological state; there are morphological changes that are due to the respiratory phase. Clusters within a super cluster were often distributed within the respiratory cycle, the S1 beats in each cluster belonging to a different range of respiratory phases. The results further support the findings of Amit et al. [16] which were found on healthy subjects, demonstrating that the phase of the respiration

cycle (inspiration or expiration), indicated by the instantaneous breathing pressure, has a marked effect on the morphology of the heart sound signal.

Super clusters were found useful when cluster members differ in more than one dimension. Specifically, the morphology of heart sounds depends on the physiological condition of the patient (abdominal pressure), and in each such physiological condition it depends on the respiratory cycle. The result of segmenting data to super clusters was characterized by the division of a single class label into several super clusters. This indicates that super clustering was able to uncover physiological changes that are not marked by class labels. Class labels reflect only external observations on the patient's state, and thus did not accurately describe the full physiological states during the surgery.

Stability in morphology due to physiological state was observed. The length of a super cluster varied from a few second during frequent position changes, to over 5 min during surgery. This indicates that a constant physiological state induces a constant set of heart sound morphologies.

The super clustering algorithm was found to be an essential step in characterizing physiological states based on morphological clustering, as it enables us to separate the variability of the morphology into the two basic causes of that variability.

In summary, the framework we introduced analyzed heart sounds characterized by multi-level variability caused by physiological events as well as the respiratory cycle. It enabled a clear separation between morphological changes caused by the respiratory cycle, and those caused by physiological changes such as insufflation.

This framework is general, and can be used to analyze different kinds of data characterized by multi-level variability in time. In this paper the framework was demonstrated on heart sounds recorded from patients undergoing laparoscopic surgeries. In a thesis by S. Kofman, it was also tested on a data set of heart sounds recorded from patients during hemodialysis, and showed good classification accuracy [17]. Due to its general nature, the framework could also be used to analyze other biomedical signals (Figs. 7–9).

## References

- [1] G. Amit, Automatic Analysis of Vibro-Acoustic Heart Signals: Combining Signal Processing and Computational Learning Techniques for Non-invasive Estimation and Monitoring of cardiac Functionality, 2008.
- [2] R.W.M. Wahba, F. Beique, S.J. Kleiman, Cardiopulmonary function and laparoscopic cholecystectomy, *Can. J. Anaesth.* 42 (1995) 51–63.
- [3] G. Amit, K. Shukha, N. Gavriely, N. Intrator, Respiratory modulation of heart sound morphology, *Am. J. Physiol. Heart Circ. Physiol.* 296 (3) (2009) H796–H805.
- [4] M.E. Tavel, *Clinical Phonocardiography & External Pulse Recording*, 3rd ed., Year Book Medical Publishers Inc., Chicago, 1978.
- [5] M. Rangayyan, Rangaraj, *Biomedical Signal Analysis*, IEEE Press Series in Biomedical Engineering, 2002.
- [6] T. Reed, Heart sound analysis for symptom detection and computer-aided diagnosis, *Simul. Model. Pract. Theory* 12 (2) (2004) 129–146.
- [7] W. Myint, B. Dillard, An electronic stethoscope with diagnosis capability, in: *Proceedings of the 33rd IEEE SSST*, 2001, pp. 133–137.
- [8] T. Olmez, Z. Dokur, Classification of heart sounds using an artificial neural network, *Pattern Recognit. Lett.* 24 (2003) 617–629.
- [9] C. Gupta, R. Palaniappan, S. Rajan, S. Swaminathan, S.M. Krishnan, Segmentation and classification of heart sounds, in: *CCECE/CCGEI*, 2005, pp. 1674–1677.
- [10] C. Gupta, R. Palaniappan, S. Swaminathan, S. Krishnan, Neural network classification of homomorphic segmented heart sounds, *Appl. Soft Comput.* 7 (2007) 286–297.
- [11] D. Gill, N. Gavriely, N. Intrator, Detection and identification of heart sounds using homomorphic envelopment and self-organizing probabilistic model, *Comput. Cardiol.* 32 (2005) 957–960.
- [12] D. Boutana, M. Djeddi, M. Benidir, Identification of aortic stenosis and mitral regurgitation by heart sound segmentation on time-frequency domain, in: *Proceedings of the 5th ISISPA*, 2007.
- [13] Z. Dokur, T. Olmez, Heart sound classification using wavelet transform and incremental self-organizing map, *Digit. Signal Process.* 18 (2008) 951–959.
- [14] T. Olmez, Z. Dokur, Feature determination for heart sounds based on divergence analysis, *Digit. Signal Process.* 19 (2009) 521–531.
- [15] P.M. Bentley, P.M. Grant, J.T.E. McDonnell, Time-frequency and time-scale techniques for the classification of native and bioprosthetic heart valve sounds, *IEEE Trans. Biomed. Eng.* 45 (1) (1998) 125–128.
- [16] G. Amit, N. Gavriely, N. Intrator, Cluster analysis and classification of heart sounds, *Biomed. Signal Process. Control* 4 (2009).
- [17] S. Kofman, Discovery of Multiple Level Heart-sound Morphological Variability Resulting from Changes in Physiological States, 2009.
- [18] J.L. Joris, D.P. Noiro, M.J. Legrand, Hemodynamic changes during laparoscopic cholecystectomy, *Anesth. Analg.* 76 (1993) 1067–1071.
- [19] S.Z. Goldhaber, G. Piazza, The acutely decompensated right ventricle: pathways for diagnosis and management, *Chest* 128 (3) (2005) 1836–1852.
- [20] T. Hastie, R. Tibshirani, J. Friedman, *The Elements of Statistical Learning*, Springer, 2009.
- [21] C. Romesburg, *Cluster Analysis for Researchers*, Lulu Press, North Carolina, 1984.